NIH-PA Author Manuscript

NIH-PA Author Manuscript

NIH-PA Author Manuscript

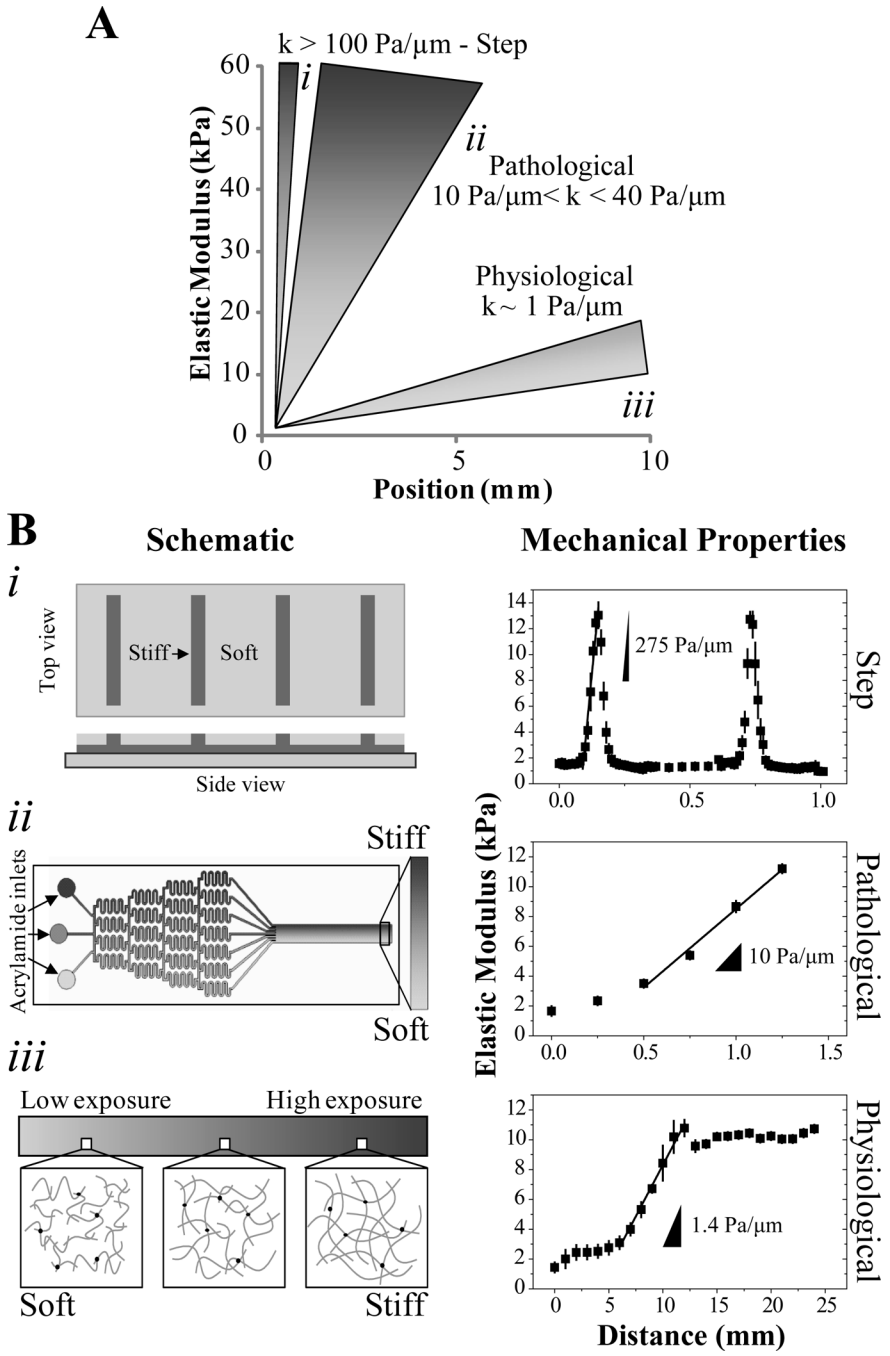

Figure 1.

(A) Schematic representation of step (*i*), pathological (*ii*), and physiological (*i*) stiffness gradients. (B) Three separate PA systems were developed to generate mechanical gradients of varying strength and of defined range spanning ~1–10 kPa. (*i*) At left is a schematic of a two-stiffness hydrogel where 500 μm wide regions of soft PA alternate with ~100 μm wide strips of stiff hydrogel producing a stripped stiffness profile. At right, there is a plot of stiffness with position, indicating that the sharp transitions between soft and stiff regions create gradients of >100 Pa/μm, n=4 gels. (*ii*) At left is a schematic of a microfluidic mixer that splits and recombines polymer solutions to generate a smooth gradient from discrete inputs. Photopolymerization of the solution in the outlet channel yields a PA hydrogel with a

uniform, one-dimensional pathological stiffness gradient of 10 Pa/μm as indicated at right, n=3 gels. (*iii*) A photomask decreasing in transparency from 100 to 30% modulates the intensity of UV that reaches the polymer solution, leading to changes in polymer chain length as illustrated at left resulting in a UV transmission gradient. This results in PA substrate with a ~1 Pa/μm mechanical gradient as shown at right, n=3 gels.

NIH-PA Author Manuscript
NIH-PA Author Manuscript
NIH-PA Author Manuscript

NIH-PA Author Manuscript

NIH-PA Author Manuscript

NIH-PA Author Manuscript

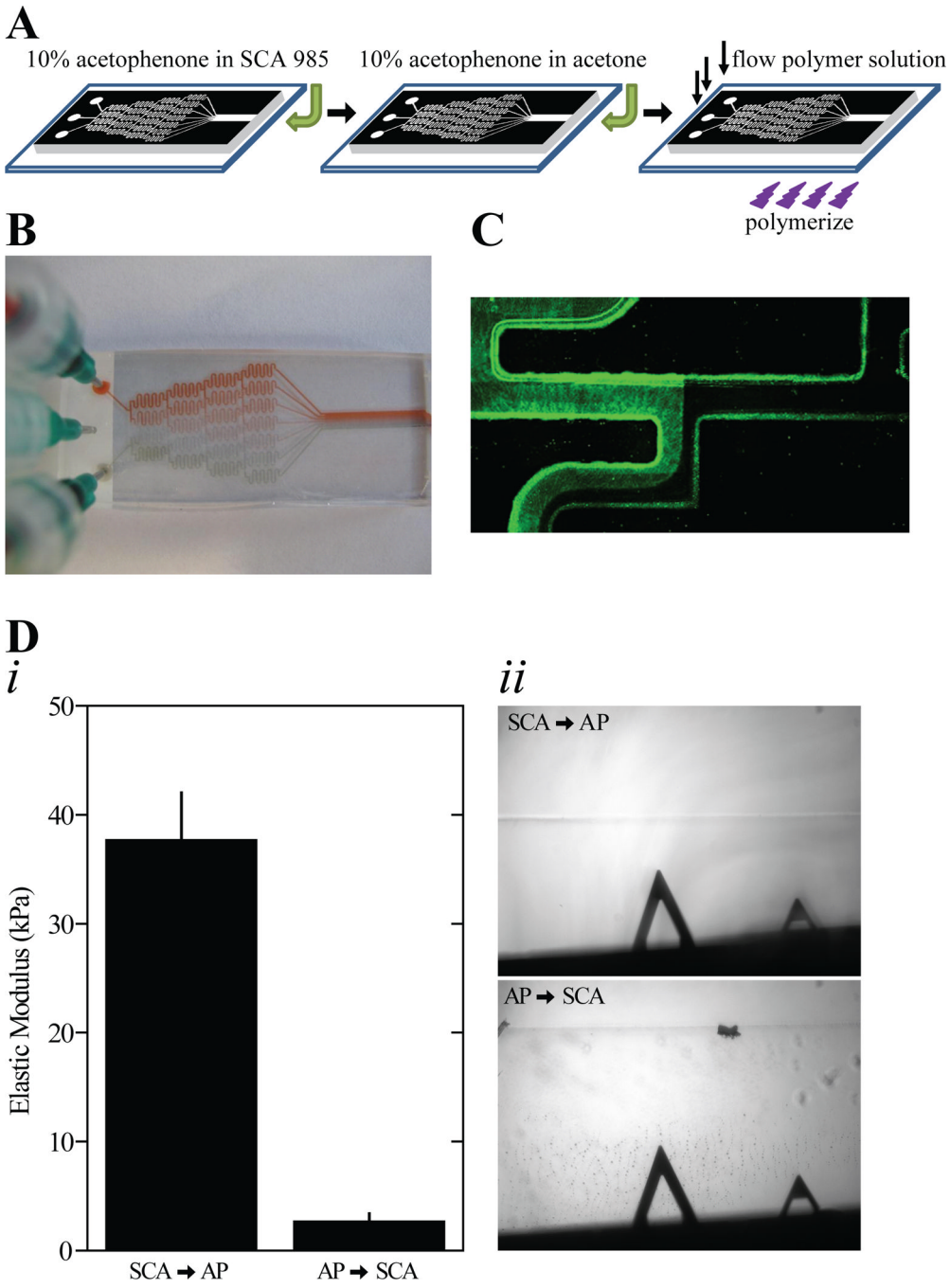

Figure 2.

(A) Schematic of the microfluidic gradient generator preparation process. (B) Image of the microfluidic gradient generator with inlets containing red, green, or no food coloring in water to visualize mixing in the channel. (C) Magnified fluorescent image of active flow in the microfluidic gradient generator at a branch point. The left inlet contains EosinY. (D) A solution was polymerized in the outlet of the gradient generator with acetophenone dissolved in SCA 985 or acetophenone dissolved in acetone and SCA 985 subsequently added. (*i*) Hydrogel stiffness is shown for the indicated order of adding acetophenone and SCA 985 to the gradient generator output channel. Error bars depict standard deviation. Measurements in triplicate were made at 6 distinct positions, n=3 gels. (*ii*) Phase contrast

images are shown of the hydrogel edge when either SCA 985 or acetophenone was added first in the preparation process.

NIH-PA Author Manuscript
NIH-PA Author Manuscript
NIH-PA Author Manuscript

NIH-PA Author Manuscript
NIH-PA Author Manuscript
NIH-PA Author Manuscript

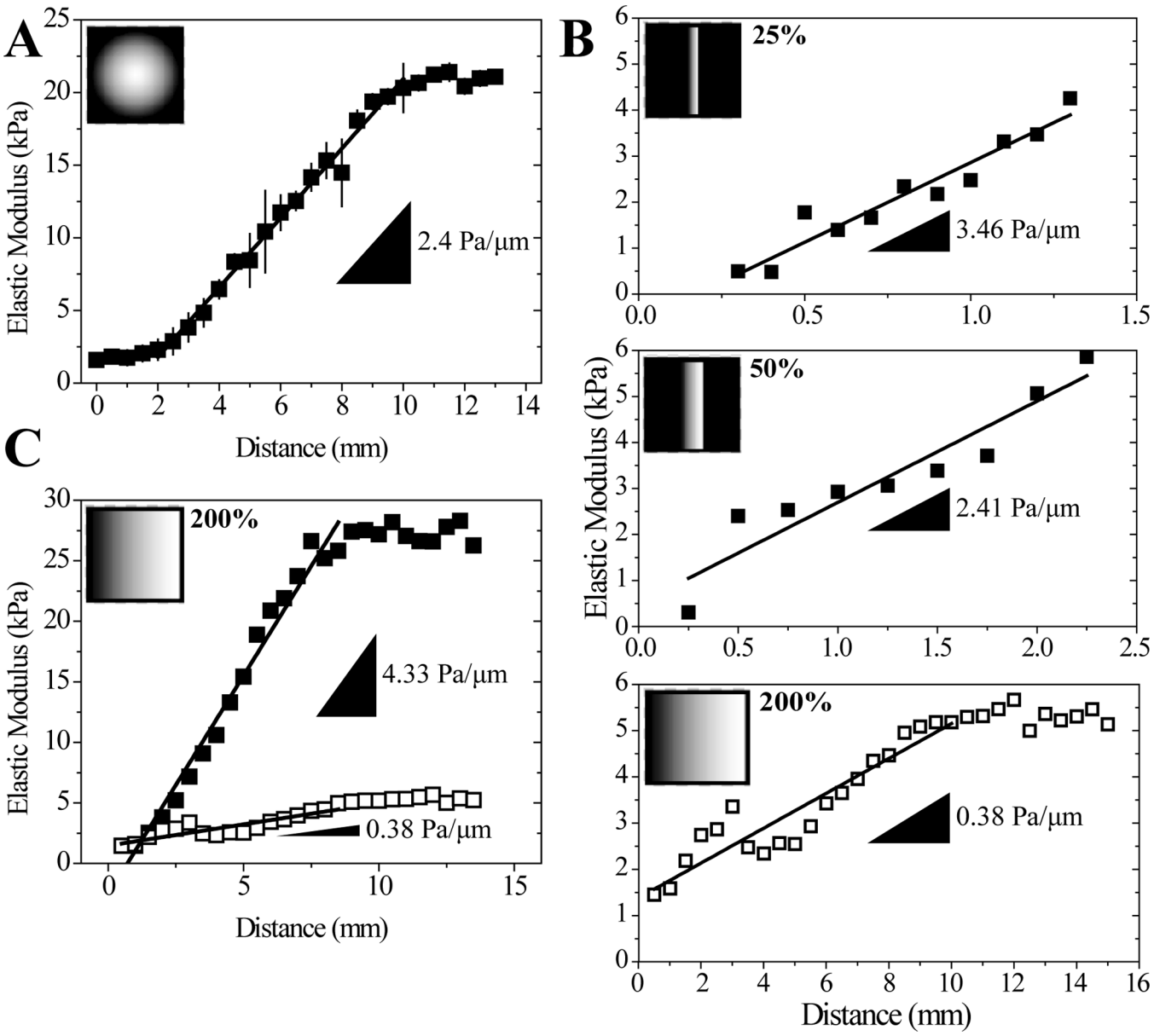

Figure 3.

(A) Gradients generated using a radially symmetric mask and a solution containing 10% acrylamide, 0.3% bis-acrylamide, and 0.5% irgacure as the initiator. n=4 gels (B) Gradients produced with the same polymer solution (10% acrylamide, 0.1% bis-acrylamide) but using photomasks where the opacity gradient was scaled to 25%, 50%, or 200% of the distance used in Figure 1B*ii*, n=1. (C) Two different gradients made with the same photomask but different polymer solutions. Closed squares: 10% acrylamide and 0.3% bis-acrylamide, open squares: 10% acrylamide, 0.1% bis-acrylamide, n=1. Insets (A)–(C): Photomask images used for gradient fabrication with indicated photomask gradient distance relative to the photomask in Figure 1B*ii*.

NIH-PA Author Manuscript

NIH-PA Author Manuscript

NIH-PA Author Manuscript

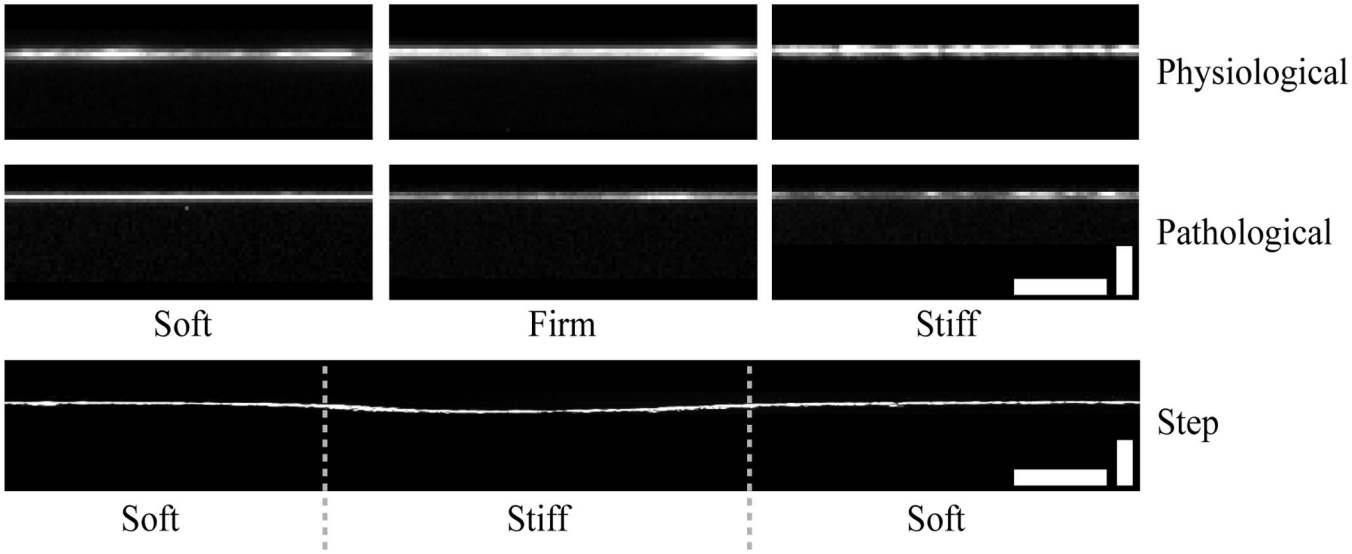

Figure 4.

Representative confocal cross-sections of each hydrogel system with fluorescently-labeled human plasma fibronectin. Each physiological gradient and pathological gradient image was averaged over 13 overlapped fluorescent cross-sections and repeated at least twice. Scale bars are 25 μm (horizontal) and 5 μm (vertical) for the physiological and pathological gradients and 25 μm (horizontal) and 20 μm (vertical) for step gradient.

NIH-PA Author Manuscript
NIH-PA Author Manuscript
NIH-PA Author Manuscript

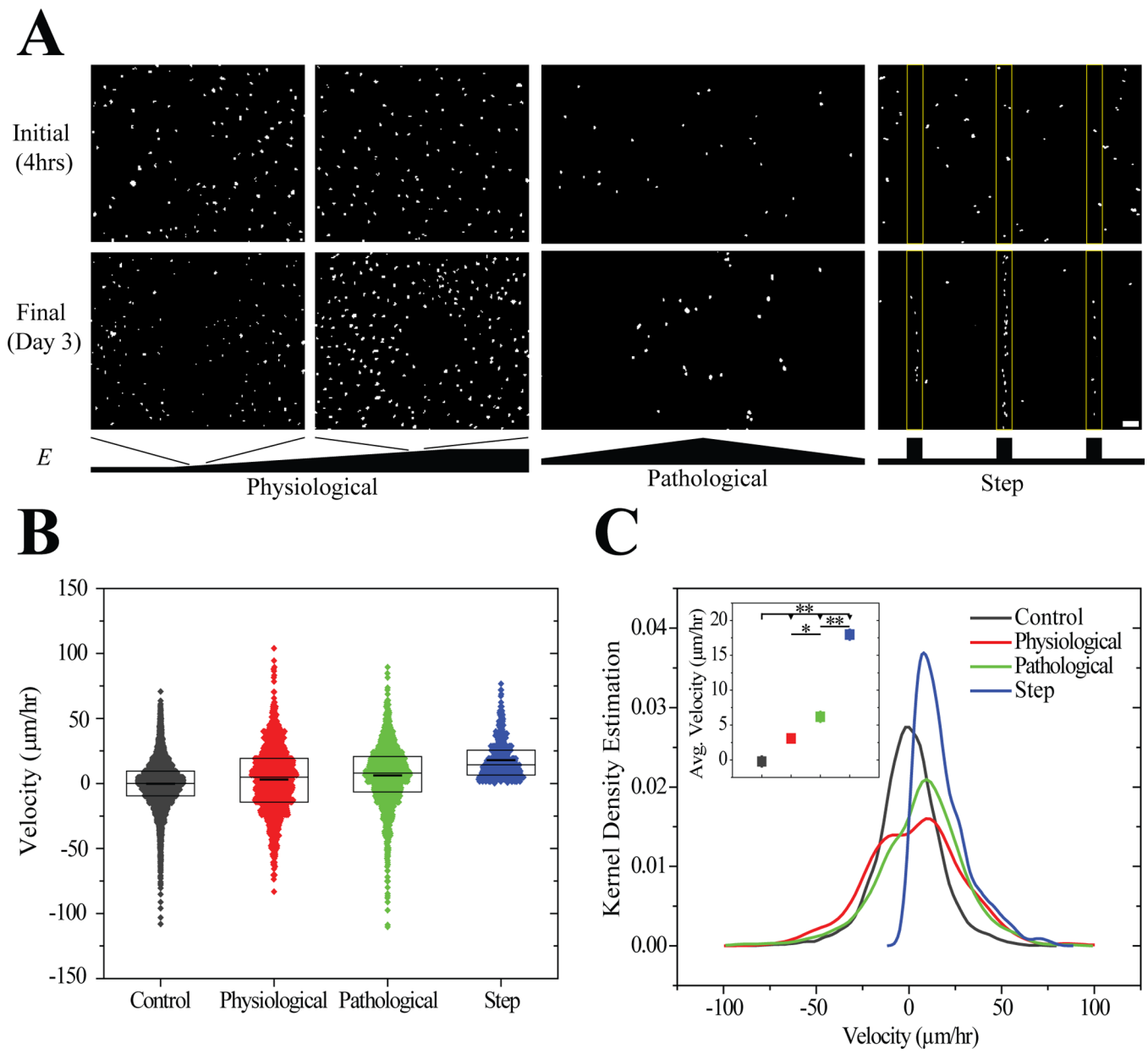

Figure 5.

(A) Thresholded images of Hoechst-stained MSCs on physiological (1.4 Pa/μm), pathological (10 Pa/μm), and step gradients (275 Pa/μm) 4 hours and 3 days after plating. Scale bar is 100 μm. (B) Velocities of migrating MSCs in the direction of the gradient determined from tracking live cells using time-lapse microscopy on physiological, pathological, and step gradients. Boxes indicate median, 25th, and 75th percentile and the thicker line indicates the average. (C) Kernel density estimation of cell velocities on the three gradient systems and average ± standard error of cell migration velocity for each system (inset). * p-value < 10^{-2}, ** p-value <10^{-5}. For step gradient, n=450 independent velocities. For physiological and pathological gradients, n>1300 independent velocities. Data were obtained from 3 biological replicates.

NIH-PA Author Manuscript
NIH-PA Author Manuscript
NIH-PA Author Manuscript

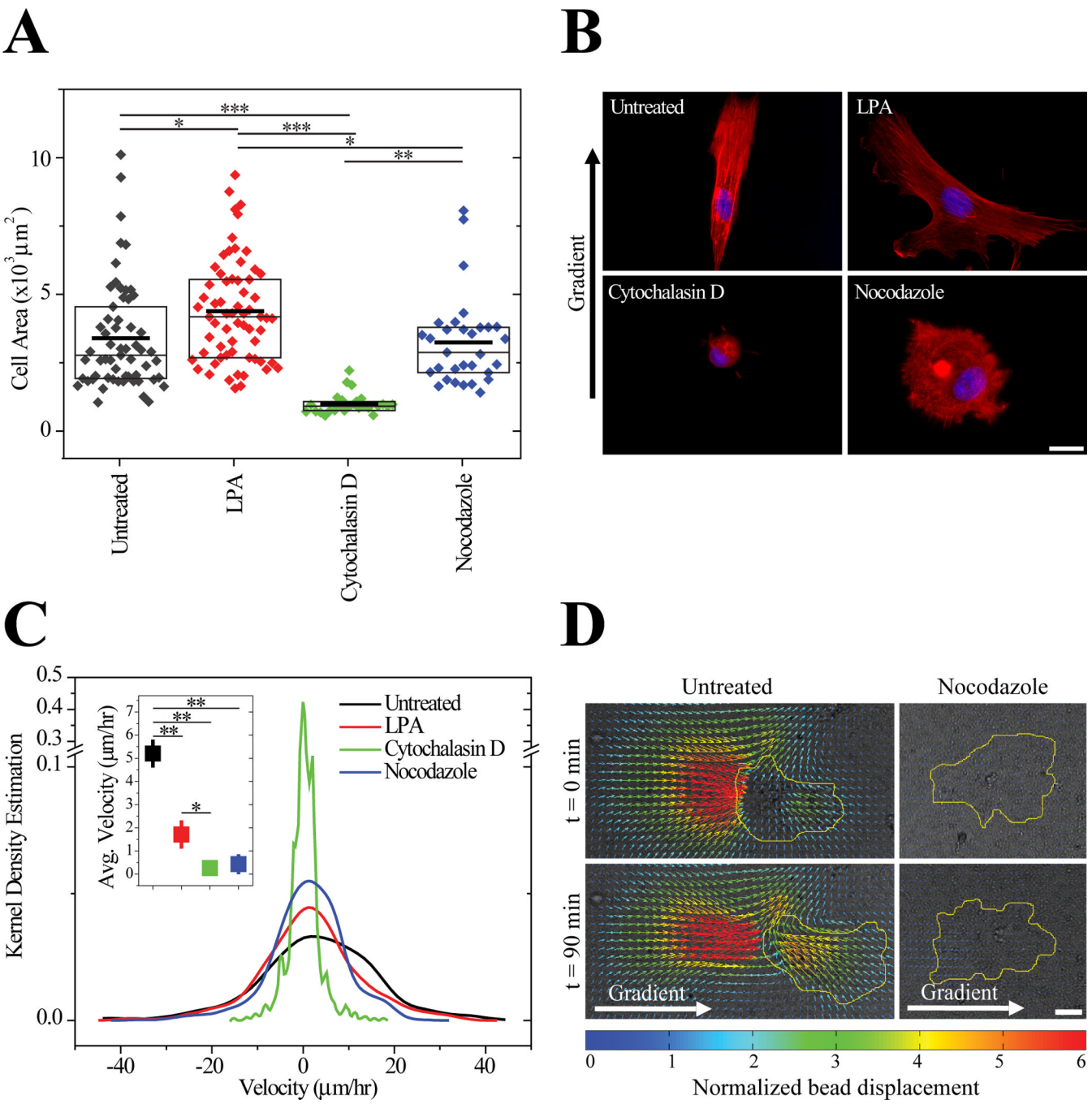

Figure 6.

(A) Spread area of MSCs on gradients either untreated (gray) or treated with lysophosphatidic acid (red), cytochalasin D (green), or nocodazole (blue) after 3 days. Boxes indicate median, 25th, and 75th percentile and the thicker line indicates the average. n>27 cells for each condition. (B) Nuclei (blue) and actin (red) of MSCs stained after 3 days in culture with inhibitors. Scale bar is 20 μm. (C) Migration of untreated and inhibitor treated MSCs on hydrogel with a pathological gradient of 8.7 ± 1.9 Pa/μm and range of 1 to 12 kPa. Inset depicts average ± standard error of cell migration velocity for each condition. For each condition, n>460 independent velocities. Data were obtained from 2 biological replicates. (D) Displacement maps of fluorescent particles embedded in the hydrogel obtained using

particle image velocimetry for untreated and nocodazole-treated cells. Brightfield images and cells contours in yellow are overlaid with the displacement maps. Gradient is from left to right. Scale bar is 30 μm. * p-value < 10^{-2}, ** p-value <10^{-5}.

NIH-PA Author Manuscript
NIH-PA Author Manuscript
NIH-PA Author Manuscript